INTERNATIONAL ATOMIC ENERGY AGENCY
UNITED NATIONS EDUCATIONAL, SCIENTIFIC AND CULTURAL ORGANIZATION
INTERNATIONAL CENTRE FOR THEORETICAL PHYSICS
I.C.T.P., P.O. BOX 586, 34100 TRIESTE, ITALY, CABLE: CENTRATOM TRIESTE

ICFA INTERNATIONAL COMMITTEE FOR FUTURE ACCELERATORS

ISTITUTO NAZIONALE DI FISICA NUCLEARE INFN

H4.SMR. 394/2

SECOND ICFA SCHOOL ON INSTRUMENTATION IN ELEMENTARY PARTICLE PHYSICS

12- 23 JUNE 1989

Playing with Multiwire Chambers

A. PENZO

I.N.F.N., Trieste, Italy

PLAYING WITH MULTIWIRE CHAMBERS

by Fabio SAULI and Archana SHARMA

1. INTRODUCTION

The purpoose of this note is to provide the basic ingredients for understanding the construction and operation of Multiwire Proportional Chambers (MWPC). A very abundant literature exist on the subject, and some major reference articles and books are listed in the last section. At this school, three completed chambers are provided for experimenting, one is given as a mounting kit to which anodes and cathodes have to be soldered, and one is kept as a set of spare parts for demonstration. All measurements will be realized using a soft x−ray radioactive source (Fe^{55} providing 5.9 keV photons), and a gas filling consisting in a mixture of argon and carbon dioxyde in an 80−20 ratio. Only measurements requiring rather simple hardware (amplifiers, oscilloscopes) will be made at the school.

2. PRINCIPLES OF OPERATION

A MWPC, in its simplest form, is made of a set of thin parallel anode wires sandwiched between two cathode planes. On application of a difference of potential between anodes and cathodes, equipotentials and lines of force develop as shown in Fig. 1.
Charges released by an ionizing radiation in the gas drift towards the electrodes under the influence of the electric field; electrons approach te anodes, where, due to the steep increase of electric field, they start experiencing inelastic collisions with the gas molecules leading to the creation of excited and ionized states. Secondary electrons produced in the gas by ionization can undergo further inelastic collisions, and this results in what is called an avalanche growth, or charge multiplication process.

The avalanche process in a MWPC is very fast, because of the short path of elctrons multiplying (ionizating collisions begin to occour usually at few tens of microns from the anode wire surface), and after a fraction of a nanosecond all electrons are collected. The positive ions left over in the trail of multiplying electrons move instead towards the cathode with a decreasing speed, roughtly proportional to the electric field strength. In their motion, they induce image charges in all surrounding electrodes, and this results in a negative signal on the anode where the avalanche originated, and in a distribution of positive induced signals in all surrounding electrodes (with amplitudes depending on the geometry). Note that the largest fraction of the detected anodic signal is produced by the receding ions; the contribution of the electrons' collection is usually negligible (less than 1% of the total charge signal).

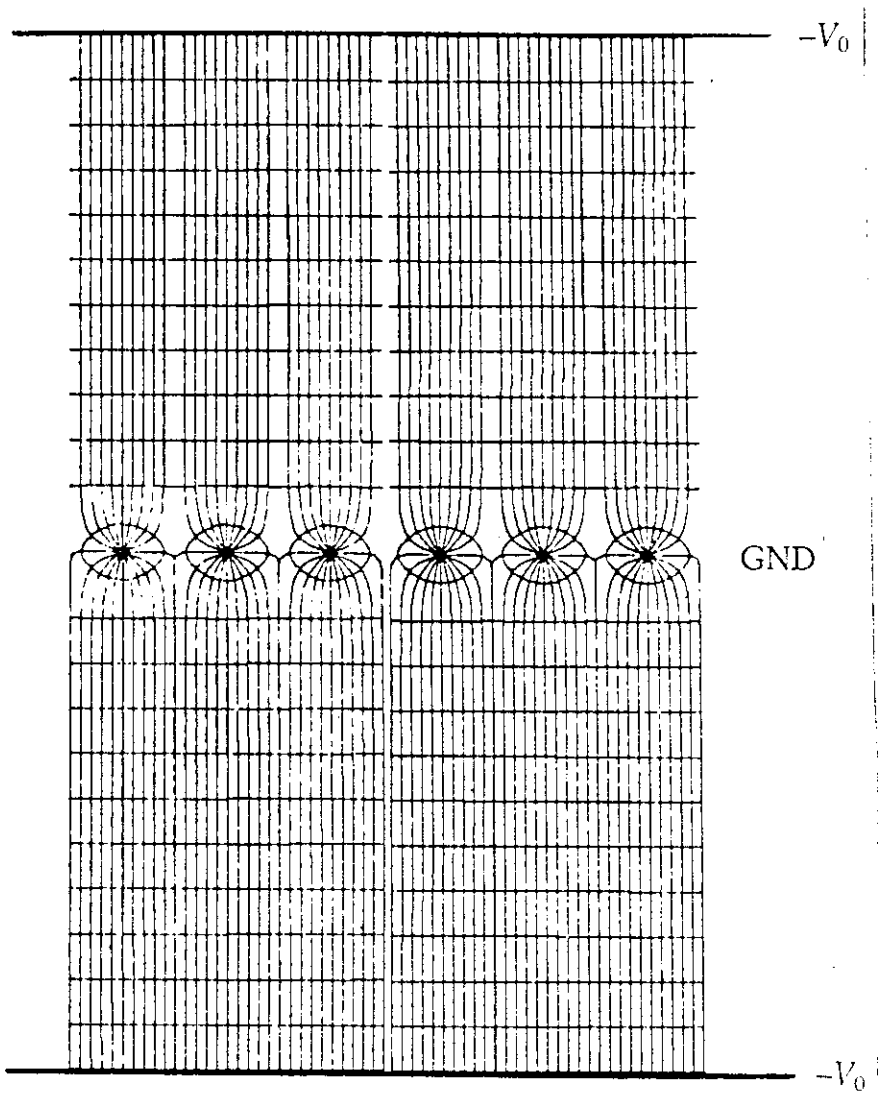

Figure 1: Schematics of a Multiwire Proportional Chamber

The electronic detection of an ionizing event can then exploit the avalanche multiplication at different levels. The simplest one is to connect to each anode wire a circuit including an amplifier, a discriminator and a latch; this will allow to detect and count all signals whose amplitude exceeds the discrimination threshold. The position accuracy is of course not better than the wire spacing, and moreover only one coordinate (perpendicular to the wire plane) is determined.

A much more powerful method of detection is possible in a MWPC having discrete cathode planes, realized with parallel wires or strips. As shown in Fig.2, the avalanche formation around an anode wire, followed

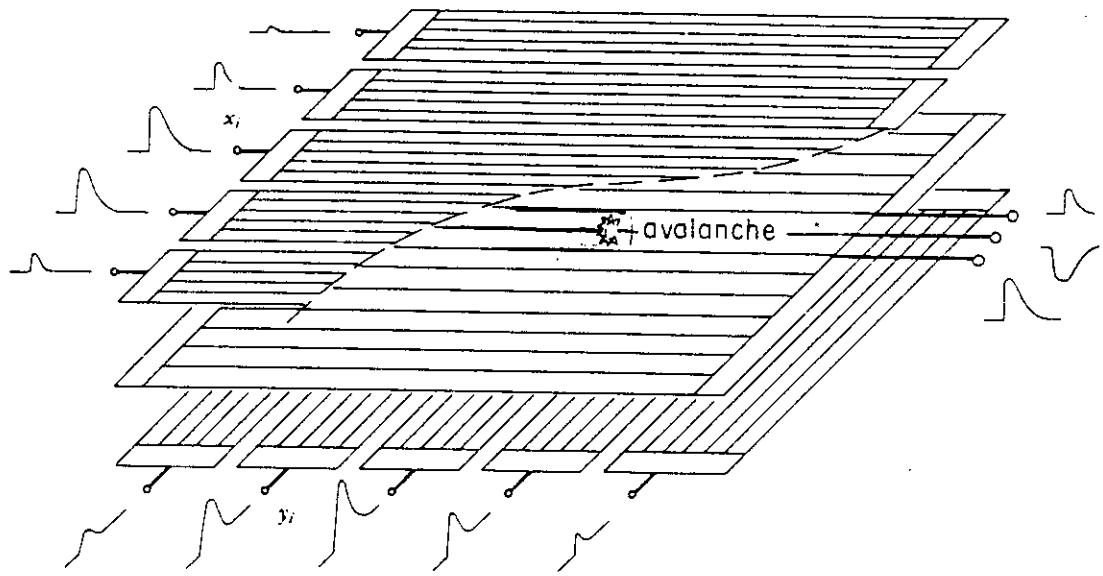

Figure 2: Direct and cathode induced signals in a MWPC

by the motion of ions towards the cathodes, results in a local induction of a positive charge profile on both cathodes. A recording, for each event, of this charge distribution on cathode strips allow to compute the center of gravity and therefore to determine the avalanche position in projection with very good accuracies (as good as 30 μm rms for a localized avalanche). Since the two sets of cathode strips can be at an angle between them and between the anodes, this method can provide three independent projections of the ionization event and is therefore very powerful; it necessitates however the use of rather expensive electronics circuits (analog to digital conversion on all wires or groups of wires and a computer).

3. MECHANICAL CONSTRUCTION

The gain, efficiency, proportionality and other operating characteristics of a MWPC depend both from the mechanical parameters (wires diameter and distances, gap, etc) and from the gas filling; the parameters can be chosen so to obtain the best performance given the major experimental need (e.g. best proportionality, highest gain, optimum localization properties). Some of these choices are discussed in the quoted literature. The chambers to be described here have a design that can be considered as typical for small size MWPCs; their main characteristics are given in Table 1.

Table 1: Mechanical parameters of the MWPC used for playing

Anode wire diameter: 20 μm
Anode wire spacing: 2.54 mm
Number of anode wires: 40 (plus several guard wires)
Cathodes: stainless steel mesh, 500 μm pitch, 50 μm diameter
Gap (anode to cathode): 5 mm
Active size: 10x10 cm^2

Fig.3 shows an assembled chamber. It consists in several insulating frames holding the various electrodes, sandwitched between two metal frames that provide the necessary rigidity to the structure; thin mylar windows on each side make the chamber gas tight.

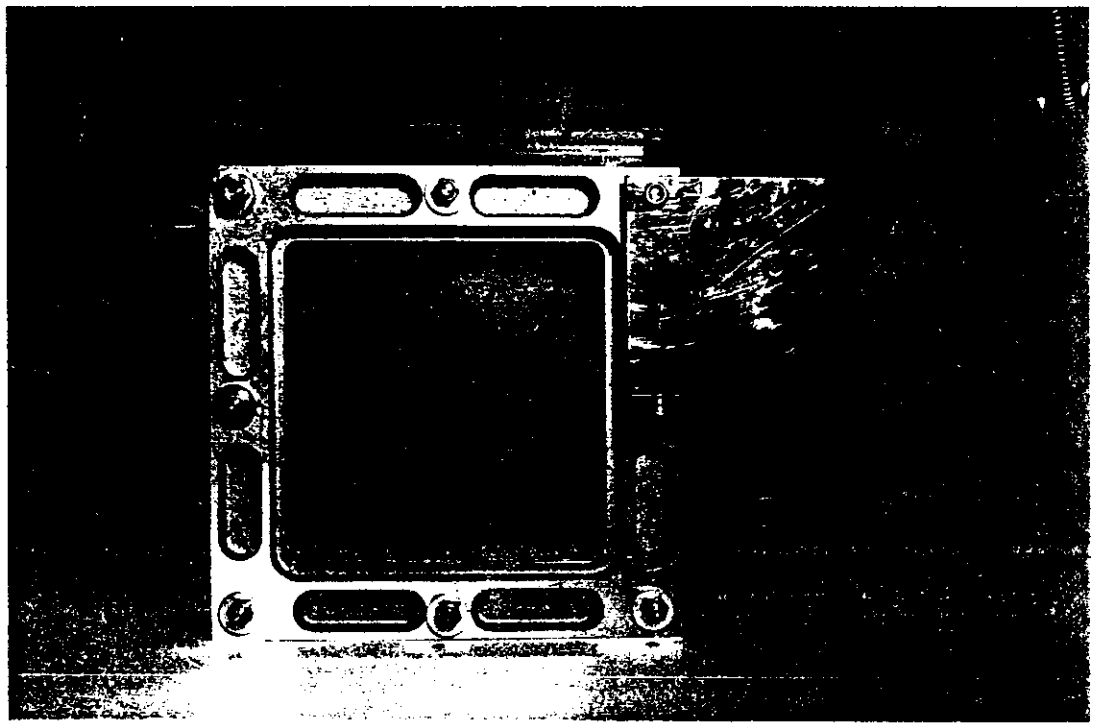

Figure 3: An assembled small size MWPC.

The gas flow is provided by two plugs on opposite sides (one is visible on the upper left). A metal pannel on the right side is used to support the high voltage connector (the MWPC is operated in this case providing a negative potential to the two cathodes, the anodes being grounded); the cathode signal can be readout on a 50 ohm plug, connected to the electrode through a high voltage capacitor. Note that the high voltage is never applied to the electrodes directly, but through a high value resistor (usually 1 to 10 Mohm) to limit the current in case of breakdown. On the upper

side, two printed circuit board connectors allow to keep the anode wires at a ground potential, and if equipped with suitable plugs to extract the signal from the whole anode plane or from individual wires.

All internal frames are realized on high−quality machined fibreglass; each frame has suitable grooves to receive rubber O−rings that guarantee gas tightness by compression. The chamber is assembled with bolts and nuts, visible in the picture; to avoid internal breakdowns with the high voltage electrodes, the (grounded) bolts are inserted in fibreglass insulating cylinders. The two exterior metal frames, aside from providing the necessary rigidity and flatness of the assembly, are also useful to establish a good ground potential reference for the chamber and the electronics.

The construction of individual electrodes is illustrated in the following pictures. Fig.4 shows the frame that will hold the cathode mesh; a single−side printed circuit board, shown at the right, is glued with epoxy into the grooves of the frame, and the interior is cut flush with the frame to provide a cornice to which a stretched mesh can be soldered. Electrical contact to the electrode is provided through the protruding tongue.

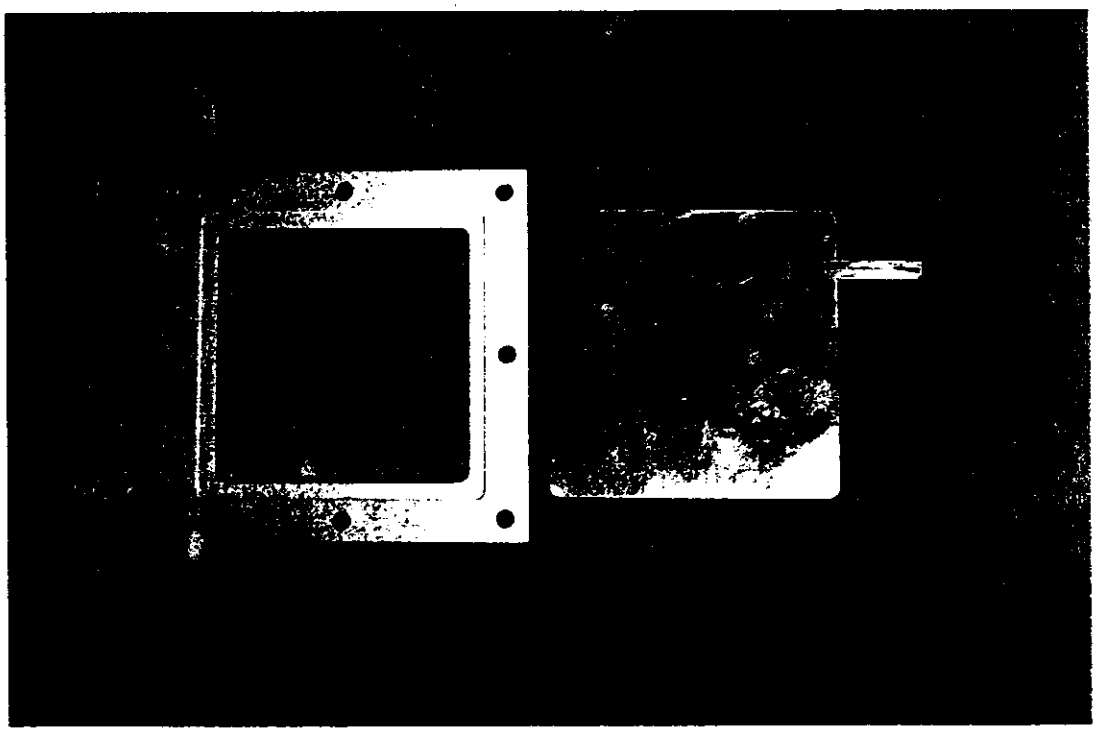

Figure 4: Fibreglass frame and printed board inset for a cathode.

The anode planes are realized stretching thin wires, by hand or with the help of a weaving machine, and soldering them to printed circuit boards glued to the frames (see Figs.5 and 6).

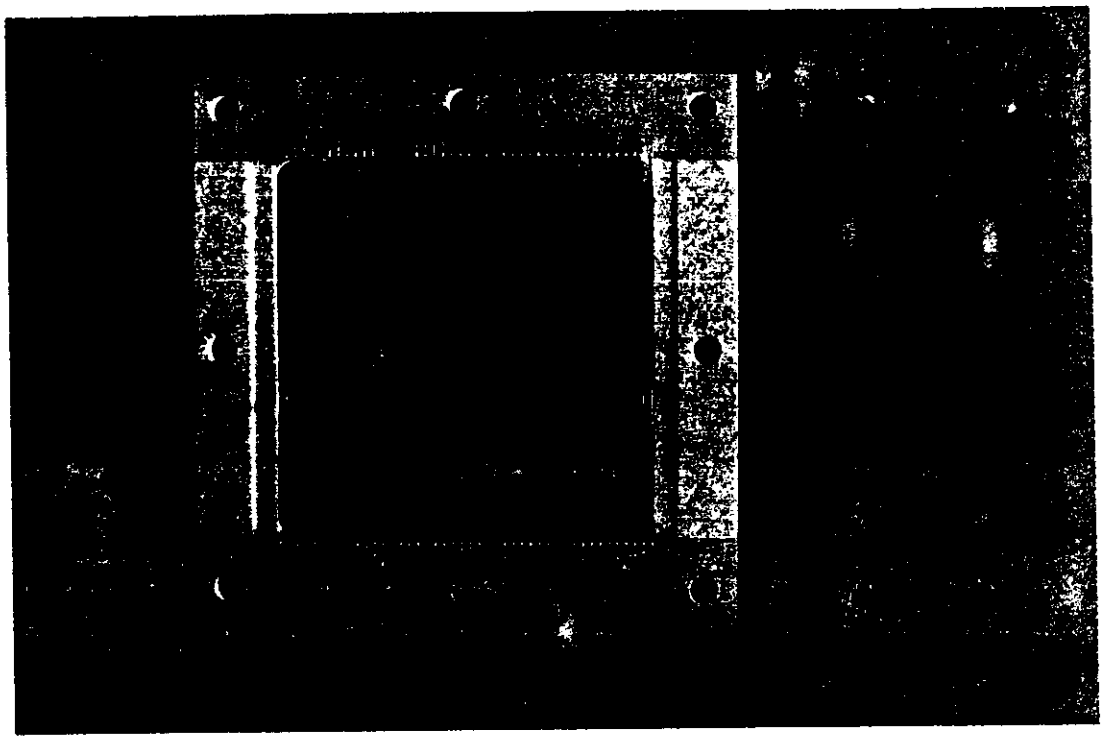

Figure 5: A wired anode plane.

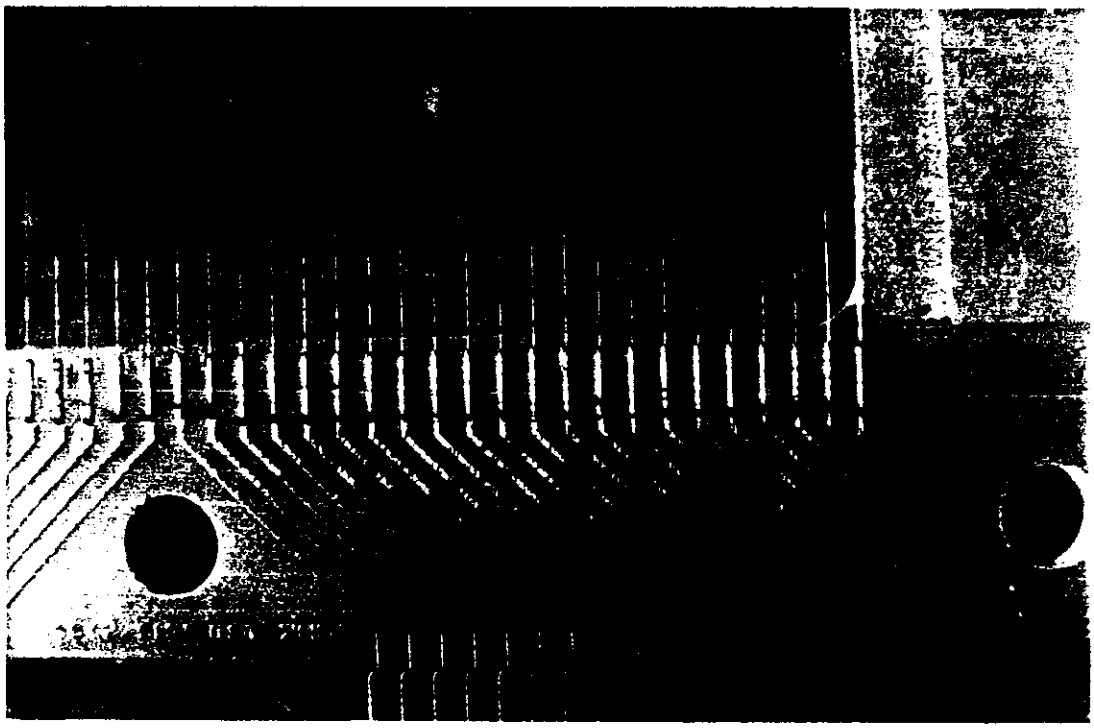

Figure 6: Detailed view of the anode wires and p.c. board.

Needless to say, the quality of soldering and the uniformity of tensioning the wires are essential ingredients to obtain a working chamber. For the 20 μm diameter gold−plated tungsten wire used, the maximum safe tension is around 60 grams (above 80 grams, the wire would permanently stretch or break). The printed circuit board used for signal outputs is visible in the detailed picture of Fig.6. To avoid edge discharges (generated by high electric fields close to insulators), the diameter of the last wires on the two sides of the wire plane is increased. In the chamber illustrated, we have used three wires with diameters of 50, 70 and 100 μm; the last two wires on each side are ganged together.

Signals can be readout from each anode wire, and for the cathode meshes, using suitable amplifiers. For this school, we have available for each chamber a two−channel bipolar amplifier, allowing to detect (with the help of an oscilloscope) both the negative anode signal an the positive cathode signal; SINCE THE AMPLIFIER IS INVERTING, ONE SHOULD REMEMBER THAT REAL POLARITIES ARE OPPOSITE OF WHAT IS SEEN. The schematics of the electronic circuit is shown in Fig.7; it makes use of a fast integrated circuit operational amplifier with some additional components. The circuit is mounted as a charge amplifier, with a time constant that can be adjusted externally with a potentiometer (from a few hundred nsec to several μsec). The two pairs of diodes at the input act as fast switches for high voltage transients, ant help protecting the circuit against overloads due to accidental discharges in the detector.

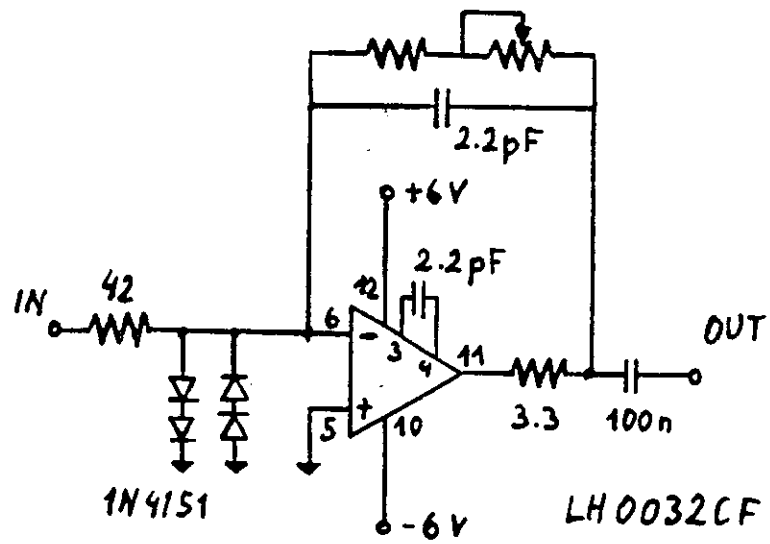

Figure 7: Electronic circuit of the inverting charge amplifier.

The typical sensitivity of the amplifier is of 300 mV per pC, meaning that a input charge of one pC will result in an output signal of 300 mV, as seen on a 50 ohm load at the oscilloscope (but, remember, inverted in sign).

4. FIRST TIME POWERING OF THE CHAMBERS

This section describes varicus measurements that can be realized with the MWPC and a few electronics components. The gas filling chosen, for simplicity and safety reasons, is a mixture of argon and CO_2 in a 80−20 ratio; this mixture can lead to instable behaviour at large gains, and cannot in general be recommended for large systems where one could have accidental discharges and breakdowns. A favored mix would be then argon with 20 or 30% of an hydrocarbon (methane, ethane,...), resulting in general in a much safer operation (see the bibliography).

In our case, to avoid (hopefully) fatal breakdowns in the chambers and in your career as physicist (unless you convert to theoretical physics), there will be a MAXIMUM ALLOWED VOLTAGE of 2.6 kV that should never be exceeded. It is indeed recommended not to operate the chamber above 2.5 kV for extended periods of time.

WARNING:
DESPITE THEIR NAME, ACCIDENTS ARE SELDOM ACCIDENTAL
APPLYING A VOLTAGE EXCEEDING THE MAXIMUM SAVE VALUE
CAN (AND IN GENERAL WILL) RESULT IN DESTRUCTION OF
THE CHAMBER AND OF THE AMPLIFIER

Several interchangeable connectors are provided to allow detection of the signals on the anode wires; one groups all twenty wires in one connector together, another allows to detect signals on a single wire and on its neighbour. UNDER NO CIRCUMSTANCES should the high voltage be applied to a chamber in which an electrode is floating, i.e. BOTH cathodes should receive the (negative) high voltage, and ALL wires should be at ground potential. Grounding can be done directly, through a resistor or through the amplifier. It is a good practice to solder a high value resistor (100 kohms or so) permanently to ground on all contacts to be connected to an amplifier; this prevents damaging the amplifier with any stored energy in a floating wire. Of course this can be done only if the amplifiers' characteristics are not modified by the grounded resistor (this is our case).

The chamber has been then installed and flushed with gas for at least an hour, to make sure that all air and pollutants (cleaning fluids, technician's cigarette smoke) have been removed from the inside. We have connected the chamber to the high voltage power supply (still OFF!), installed and powered the amplifier, connected a group of anode wires (one full connector) to its imput and wired the output to the oscilloscope. We are ready to go, according to the following guidelines.

1. Verify proper connection of the chain chamber/amplifier/oscilloscope. The simplest way is to touch the anode connector on the signal side (no danger: the HV

is still off!). This should induce enought high frequency noise to verify that the amplifier works, the scope is triggered by small signals and we are looking at an active channel (select a 10 − 20 mV/div, 1μsec/div sensitivities, internal trigger on positive signals).

2. Install the Fe^{55} source in front of the section of the chamber on which we expect to detect signals, and open the collimator.

3. On the HV supply, set the voltage control to zero and the current limiter to minimum (usually a few μA). Switch the HV unit on.

4. Slowly increase the voltage, continuously watching the scope and adjusting the trigger level; positive signals should begin to appear at around 2.1 kV, and at 2.2 kV one should get about 40 mV. If no signal is seen at 2.3 kV, or if there is any indication of failure (large signals that set in and remain on removal of the source, current in the chamber, detected on the power supply, exceeding a few μA), stop and call for help.

5. If everyting seems OK, one can reach 2.5 kV and observe a beatiful 5.9 keV line providing a signal of about 400 mV, plus a small line at lower pulse height (the argon escape line, see later). The chamber is operating and measurements can start.

5. PLAYING WITH THE CHAMBERS

This section will describe various measurements that can be realized with the MWPC and the basic electronics provided. Of course, use of more sofisticated electronics and of a small computer would allow a much more detailed and refined work.

At first, let us examine the pulse height and shape, as directly visible on the oscilloscope (Fig.8). For this picture, and only for this, the channel polarity on the scope has been inverted (notice the downwards arrow on the bottom sensitivity scale) to show the real sign of the anode signal (remember, amplifiers are inverting!). The picture has been taken at 2.3 kV, looking at a full connector, i.e. a group of 20 wires; the main line, corresponding to the 5.9 keV photon conversion, is visible. Note the fast falling time (few tens of nsec), a convolution of the avalanche development time, the ions' early motion and amplifiers' bandwith.
The recovery, or decay time, is instead characteristic of the amplifier, as indicated, and can be varied; in the picture, it is of around 2 μsec. The faint line at about half pulse height is due to the argon escape, and corresponds to the following physical process (for more details, see the references). The 5.9 keV photon emitted by the source is converted in argon by a photoelectric process mainly on the K − shell, whose edge energy is 3.2 keV. A photoelectron of 2.7 keV is emitted, followed by either of the two competing processes: emission of a photon of energy close to but smaller than 3.2 keV (a transition from the L − shell to the K − shell), or the emis-

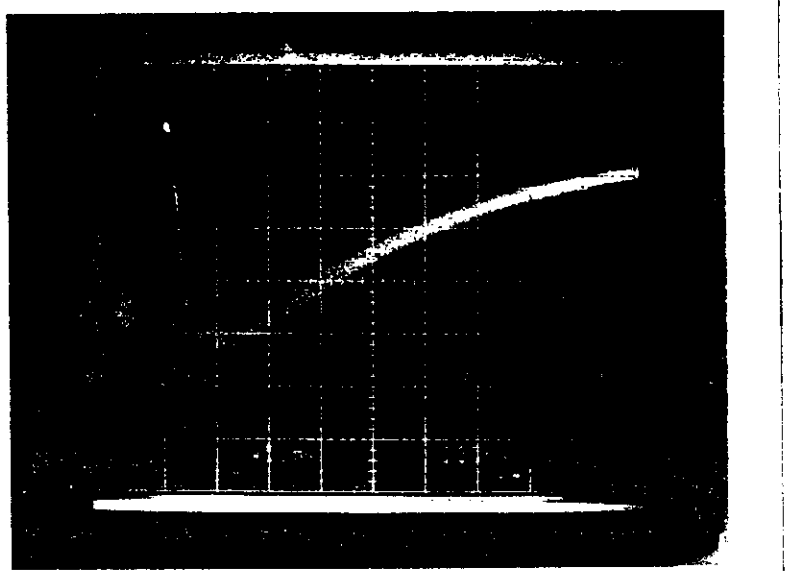

Figure 8: Anodic signal for Fe^{55}

sion of a second (Auger) electron of around the same energy. In the second case, the total ionization detected locally is close to 5.9 keV, which corresponds to the main peak. In the first case, instead, the photon can escape detection (eg, absorbed in the walls) thus giving the a detected energy of only 2.7 keV. In argon, the fluorescence yield (photoabsorption followed by emission of a photon) is only 20%, thus explaining the smaller probability of a count in the escape peak.

Note on the image that the ratio of pulse height between the two lines is roughtly what one would expect from the previous considerations, indicating that the chamber is operating in a proportional mode.

The same pattern is of course seen on the cathode planes, that detect the induced signal from the avalanche, of course with inverse polarity (positive on the cathode) and smaller amplitude (the signal is shared by various electrodes, and moreover the larger capacitance of the electrode decreases the effective charge gain of the amplifier).

Students may want to elaborate on the practical consequences of the escape phenomenon, both in term of energy resolution and of localization properties of the chamber. Also, with reference to the shape of photoionization cross sections of gases, and of noble gases in particular (see bibliography), one can discuss the choice of the gas better suited for detection of x−rays of various energies, say from a few keV up

to several tens of keV (at higher energy, the efficiency of detection in a thin gas detector becames too small).

We can now (after switching off the high voltage) replace the connector grouping all wires with that having independent outputs for two adjacent wires. The oscilloscope will be triggered on a wire, and we can observe the adjacent one as well. After application of the voltage (NOTE: start again from zero and increase slowly up to 2.3 − 2.4 kV), the pattern shown in Fig.9 should appear. Now the signals' polarities are as they appear on the scope: the upper track (sensitivity 50 mV/div) corresponds to the main signal we are triggering on, and the lower is the (positive) induced signal on the neighboring wire (sensitivity 20 mv/div).

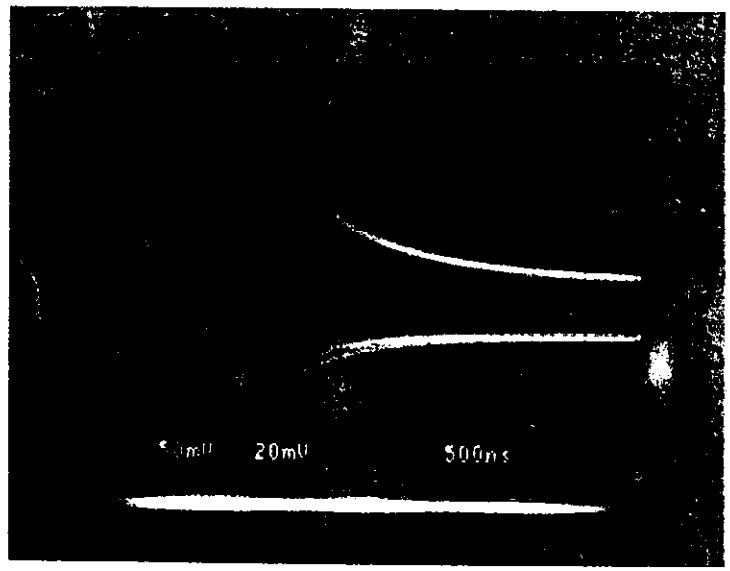

Figure 9: Direct and induced signals on two adjacent anode wires.

Note the identity of the two signals, except for their polarity and the amplitude; the induced signal is about 15% of the direct one. Since the other neighbour wire would get the same signal, this leaves for the cathodes about 70% of the induced signal, of course equally shared between the two electrodes.

A full gain curve as a function of high voltage can be measured recording on the scope the pulse height of the main line. This can be done either for a single wire or for the full group of wires; a typical result is shown in Fig.10 (remember the 2.6 kV absolute limit!). A measurement on the group of wires will provide a slightly smaller pulse height at a given voltage; based on the already given informations, the student should be able to indicate the reasons (there are two). In the figure, we have used a

semilogaritmic scale; this is because a very simple theory of avalanche growth anticipates an exponential increase of pulse height with voltage (therefore a straight line in a semilog plot). The deviation from linearity at the highest gains is due to space charge phenomena, see later.

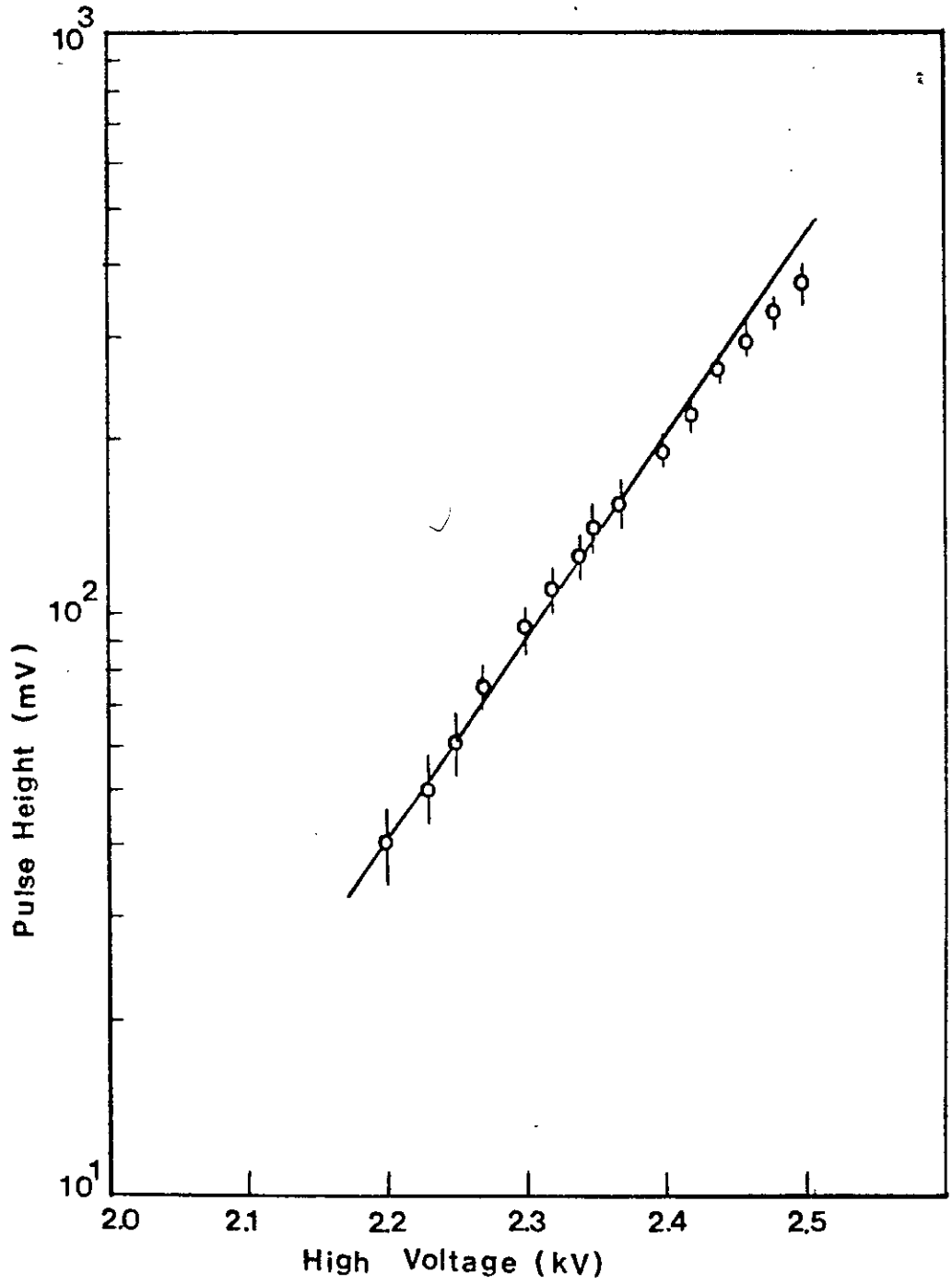

Figure 10: Pulse height vs. voltage measured on the anode plane.

Pulse height spectra can be recorded and analysed better using a pulse height analyzer. The output of the amplifier, either directly of through a shaping amplifier (depending on the characteristics of the analyser); typical pulse height spectra recorded on the group of anodes are shown in Fig.11a, b and c at increasing operating voltages (2.2, 2.5 and 2.6 kV, respectively). The sensitivity of the recorder has been adjusted so to display spectra of about the same amplitude, but of course one has to remember that the real amplitude increases tenfold from 2.2 to 2.5 kV (see Fig.10).

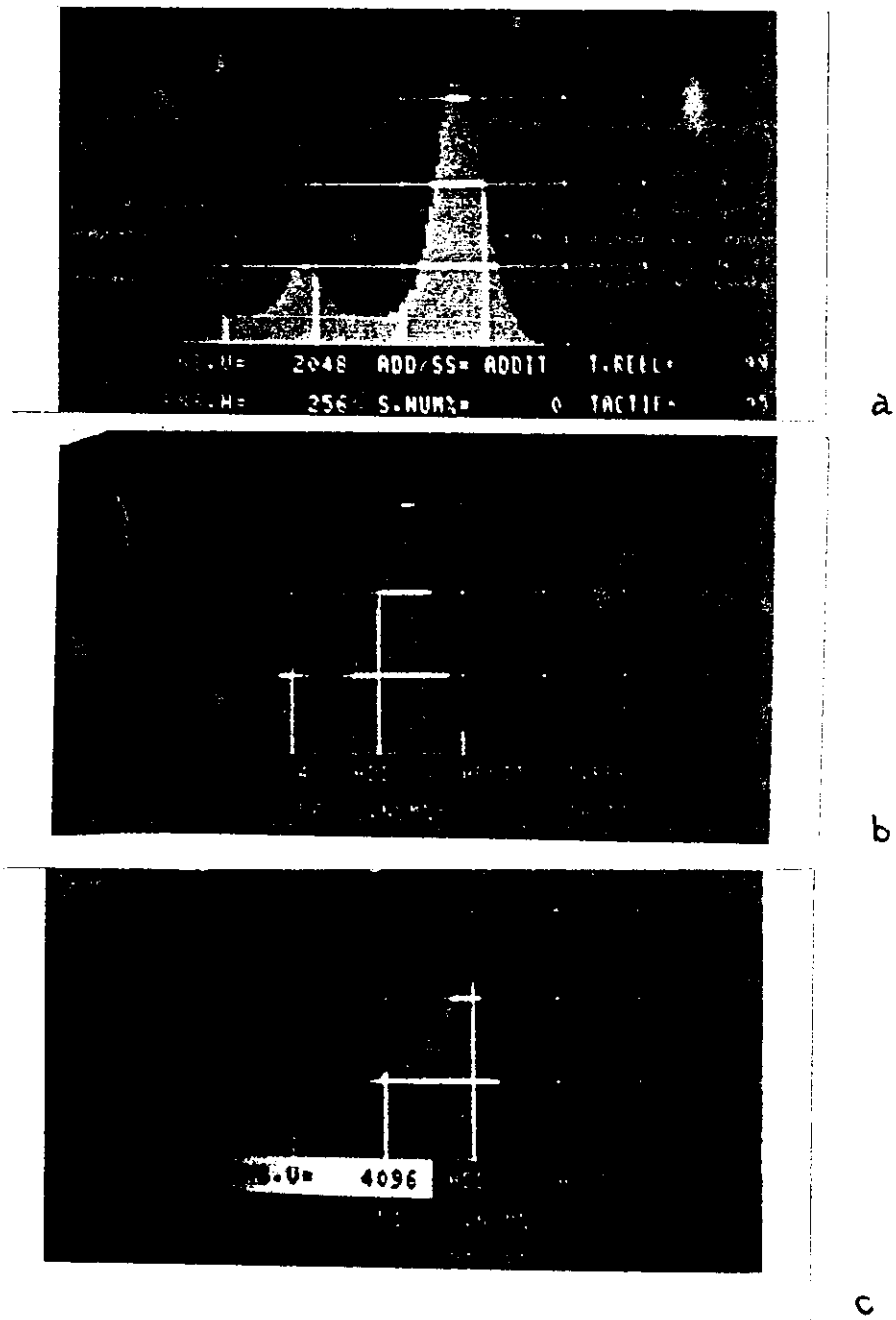

Figure 11: Pulse height spectra for Fe^{55} at increasing voltages.

The two−peak structure already discussed is evident, as is another feature: proportionality gets worse and tends to be lost at the highest gains. This is often called saturation, and corresponds to the following physical process. The growing cloud of positive ions in the avalanche tends to modify the local electric field, in the sense of reducing its value close to the surface of the anode wire. This effect is particularly important for high densities of initial ionization (large energy losses) and high gains. A decrease of the field at the anode surface has obviously as a consequence a local reduction of the effective gain for any further avalanche. Because of various dispersive effects (range in the gas of the initial photoelectron, electron diffusion during the collection etc), the time spread in the avalanche formation is such that at high operating voltages the effective gain is dynamically decreased during the multiplication process. The effect is of course larger for the higher energy losses. As a limiting case, which we cannot verify with the chambers because of the moderate quenching properties of the gas mixture used, all initial ionizations (starting with a single electron produced, say, by an ultraviolet photon in the gas) would provide the same pulse height. This is called a saturated regime.

Other modes of large gain operation can be obtained in MWPC, again depending on their geometry and gas filling: a Geiger mode, a limited streamer mode and so on (see bibliography). They have been exploited in practice whenever one does not need any kind of energy resolution, but large pulse height are a premium (reducing the electronic costs).

The last measurements to be described are the efficiency and noise rates. Using an x−ray source, there is of course no direct way to measure the absolute detection efficiency (this would be possible using charged particles, that can provide a signal both in the chamber and in a set of external scintillation counters used as a reference). The presence of a plateau however will be a good indication that all photons converting in the gas are actually detected.

To measure the detection efficiency, we will connect the output of the amplifier to a discriminator, triggering at a given voltage level, and count the rate at fixed time with a scaler. One minor technical difficulty arises from the fact that standard NIM−crate based discriminators are sensitive to negative input pulses, while the output of the amplifier is positive for the anodic signal. This can be solved using either an active linear inverter, also existing as standard NIM module, or a passive pulse transformer with unity gain. Alternatively, one can measure the efficiency on the cathode signals, but their average pulse height is of course smaller and the plateau (if any) will be shorter.

The counting rate plateau shown in Fig.12 has been measured in the following conditions. For a group of 20 anode wires (using the appropriate connector) the signar rate (estimated at the scope) has been reduced to moderate levels (a kHertz or so) collimating or changing the distance of the source (this to avoid electronic pile-ups). The output of the amplifier has been inverted with a unity gain linear amplifier, and the signal sent to a low−level fast discriminator with threshold set to minimum (−30 mV). The output logical signal, stretched to a length of around a μs or

so to avoid double triggering on long input pulses, is sent to a scaler with a preset time count (10 s or so). The counting rate per second is then recorded as a function of voltage, as shown in Fig.12 (open circles and left scale).

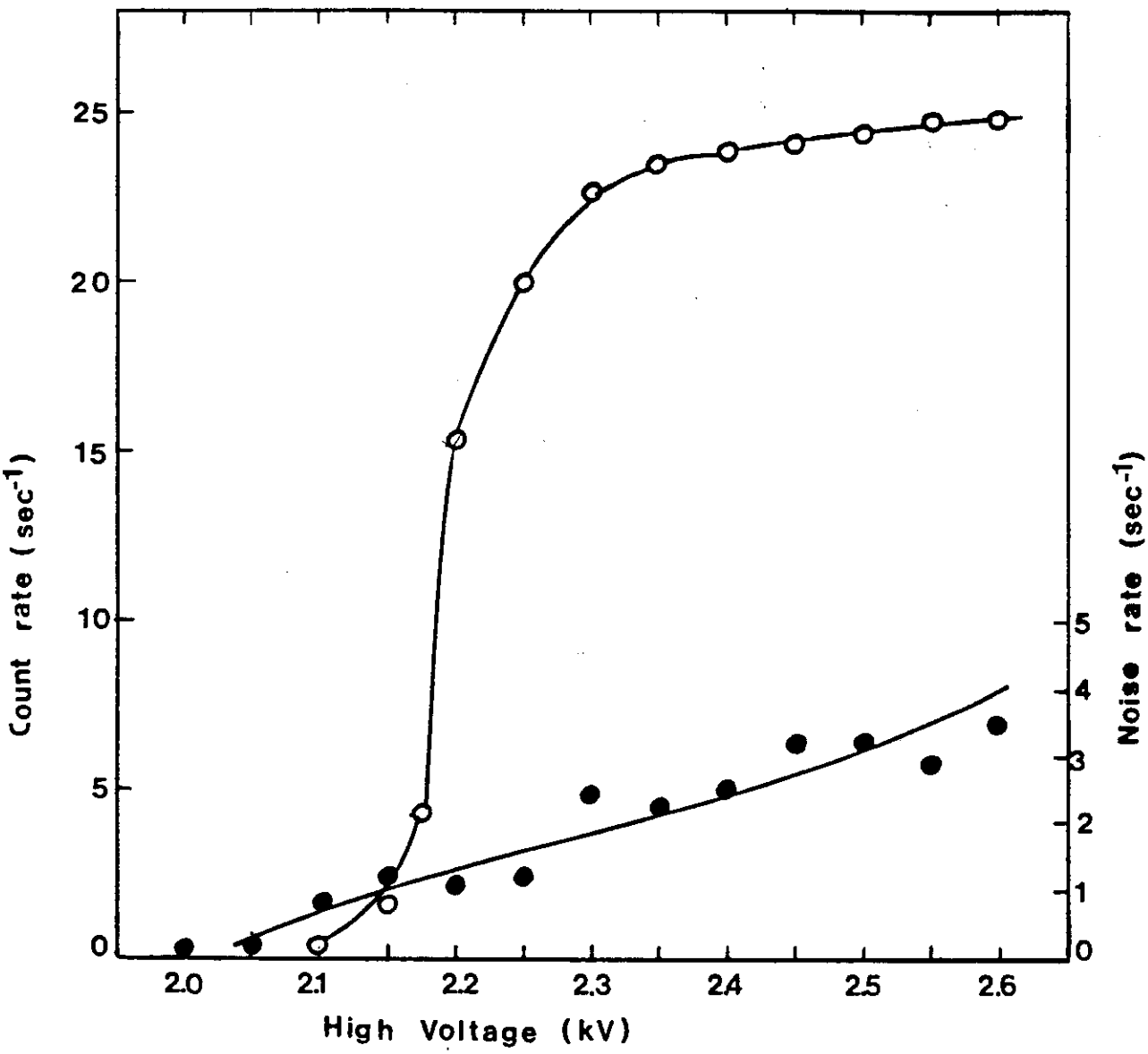

Figure 12: Counting rate plateau and noise rate as a function of voltage.

The same figure shows also the noise rate of the chamber, i.e. the counts per second when the source is removed (full points and right scale). This rate includes of

course various sources of noise: spontaneous discharges, electronics noise, natural radioactivity, cosmic rays. The students may want to estimate their relative importance. As shown, a total rate of a few counts per second on a group of 20 wires is rather small and can usually be ignored for all practical purpooses.

TO KNOW MORE ON GASEOUS DETECTORS

COUNTING TUBES, THEORY AND APPLICATIONS, by S.C.Curran and J.D.Craggs (Butterworths, London 1949)

IONIZATION CHAMBERS AND COUNTERS, by D.H.Wilkinson (Cambridge Univ.Press, 1950)

ELECTRON AND NUCLEAR COUNTERS, by S.A.Korff (Van Nostrand, New York 1955)

BASIC PROCESSES OF GASEOUS ELECTRONICS, by L.B.Loeb (Univ.of California Press, Berkeley 1961)

ELECTRON AVALANCHES AND BREAKDOWN IN GASES, by H.Raether (Butterworths, London 1964)

COLLISION PHENOMENA IN IONIZED GASES, by E.W.McDaniel (Wiley, New York 1964)

BASIC DATA OF PLASMA PHYSICS, by S.C.Brown (MIT Press, Cambridge 1967)

ATOMIC AND MOLECULAR RADIATION PHYSICS, by L.G.Christophorou (Wiley, New York 1971)

ELECTRICAL BREAKDOWN IN GASES, ed. by J.A.Rees (MacMillan, London 1973)

EVOLUTION OF THE AUTOMATIC SPARK CHAMBERS, by G.Charpak: Annu.Rev.Nuclear Sci. 20 (1970) 195

PRINCIPLES OF OPERATION OF MULTIWIRE PROPORTIONAL AND DRIFT CHAMBERS, by F.Sauli. CERN 77-09 (1077)

FLUCTUATIONS IN CALORIMETRY MEASUREMENTS, by U.Amaldi. Phys.Scripta 23 (1981) 708.

CHERENKOV RING IMAGING, by T.Ypsilantis. Phys.Scripta 23 (1981)370.

FUNDAMENTAL PROCESSES IN DRIFT CHAMBERS, by B.Sadoulet. Phys.Scripta 23 (1981) 433.

CALORIMETRY IN HIGH-ENERGY PHYSICS, by C.W.Fabjan. CERN EP/85-54 (1985).

HIGH-RESOLUTION ELECTRONIC PARTICLE DETECTORS, by G.Charpak and F.Sauli. Ann.Rev.Nucl.Part.Sci. 34 (1984) 285.

PROCEEDINGS OF THE VIENNA WIRE CHAMBER CONFERENCE 1983, ed.by W.Bartl and G.Neuhofer. Nucl.Instrum.Methods in Phys.Res. 217 (1983) 1-382.

THE TIME PROJECTION CHAMBER, ed.by J.A.Macdonald. AIP Conf.Proc.108 (Am.Inst.of Physics, New York 1984).

PARTICLE DETECTORS, by K.Kleinknecht, in Techniques and Concepts of High-Energy Physics ed.by Th.Ferbel (Plenum, New York 1981).

NEW DEVELOPMENTS IN GASEOUS DETECTORS, by F.Sauli, in Techniques and Concepts of High-Energy Physics II, ed.by Th.Ferbel (Plenum, New York 1983).

PARTICLE DETECTORS, by C.W.Fabjan and H.G.Fischer, Rep.Progr.Phys. 43 (1980) 1003.